Scientific and Technical Section

UDC 539. 4

Ab Initio DFT Study of Ideal Shear Strength of Polytypes of Silicon Carbide

Y. Umeno,[1,a] Y. Kinoshita,[2,b] and T. Kitamura[2,c]

[1] Institute of Industrial Science, The University of Tokyo, Tokyo, Japan

[2] Graduate School of Engineering, Kyoto University, Kyoto, Japan

[a] umeno@iis.u-tokyo.ac.jp, [b] yusuke-kinoshita@t02.mbox.media.kyoto-u.ac.jp, [c] kitamura@me.kyoto-u.ac.jp

Ab initio density functional calculations are performed to investigate the ideal shear deformation of SiC polytypes (3C, 2H, 4H, and 6H). The deformation of the cubic and the hexagonal polytypes in small strain region can be well represented by the elastic properties of component Si_4C-tetrahedrons. The stacking pattern in the polytypes affects strain localization, which is correlated with the generalized stacking fault (GSF) energy profile of each shuffle-set plane, and the ideal shear strength. Compressive hydrostatic stress decreases the ideal shear strength, which is in contrast with the behavior of metals.

Keywords: ideal strength, shear deformation, ab initio simulation, silicon carbide.

Introduction. Silicon carbide (SiC) possesses prominent properties such as high mechanical strength, chemical stability and large band gap energy, and has been widely used as thermal and mechanical functional material, electromagnetic functional material, etc. Detailed investigations in atomistic and electronic level are required for SiC crystals because they have a variety of polytype structures characterized by stacking sequence [1], which contributes to their interesting mechanical properties. Thus, with the aim to elucidate its mechanical deformation behavior, not only experimental studies but also theoretical approach such as atomistic modeling have been carried out [2]. *Ab initio* (first principles) calculations have also been performed [3–5] to give reliable theoretical insights to the mechanical properties of SiC around the equilibrium state. However, the investigations of the mechanical properties around highly strained conditions are indispensable for understanding of deformation behavior of crystals. Although *ab initio* investigations of the tensile properties of 3C(β)–SiC by Li and Wang [6] and of the shear by Ogata et al. [7] have brought some interesting results, this issue deserves further studies. In particular, it is important to theoretically evaluate the ultimate strength under ideal shear deformation of polytypes, which is relevant to the critical shear stress at the onset of dislocation nucleation from a pristine crystal, to understand the plasticity in the atomistic scale. Moreover, the response of the ideal shear strength to compressive stresses is worth investigating because local lattice configurations may receive shear deformation in combination with normal stresses in experiments, namely nanoindentation.

Since the mechanical behavior at atomic scale is strongly correlated with the electronic nature and it is difficult for empirical interatomic potentials to correctly represent various properties away from the equilibrium state, it is important to study the mechanical deformation by atomistic and electronic modeling, namely the *ab initio* methodology.

In this study, we perform *ab initio* calculations based on the density functional theory (DFT) to investigate the ideal shear deformation of SiC polytypes (3C, 2H, 4H, and 6H) with the aim to provide fundamental knowledge about the mechanical properties of the crystals including their behavior under highly sheared strain conditions and the ideal strength, focusing on the effect of the intrinsic polytype structure on the strain localization and the ideal strength. We further explore the effect of hydrostatic pressure on the ideal strength.

Structure of SiC Polytypes. SiC consists of tetrahedrons where vertices are occupied by silicon atoms with carbons located in the center of gravity. The crystal possesses various structures (SiC polytypes) with different stacking sequence, which are denoted in Ramsdel's notation as nX, where n is the number of layers along the c-axis per periodic cycle and X is the identifier of crystal structure (C: Cubic and H: Hexagonal). Figure 1 depicts the structures of 3C, 2H, 4H, and 6H polytypes. In this study, shear deformation on the c-plane, which is (111) in cubic structure and (0001) in hexagonal, is studied because it is associated with an important slip system of SiC. As is schematically delineated in Fig. 2, cubic (3C) and hexagonal (2H, 4H, 6H, ...) crystals have different symmetry in shear deformation due to the stacking structure [8]. Concerning shear on the c-plane, 3C–SiC has three-fold symmetry resulting in different geometrical configurations between shear deformations in and its opposite direction($[1\bar{2}1]$). On the other hand, hexagonal polytypes have six-fold symmetry in shear deformation on (0001) plane because their stacking consists of Si_4C-tetrahedrons facing opposite directions. The shear deformations in a direction and its opposite (e.g., $[01\bar{1}0]$ and $[0\bar{1}10]$) are therefore identical in hexagonal polytypes.

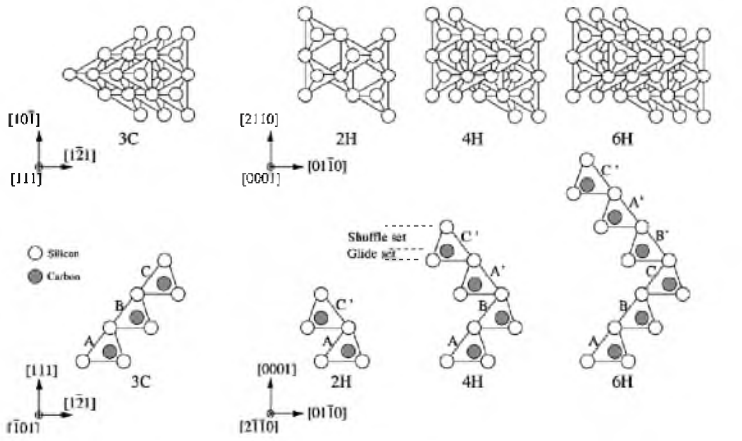

Fig. 1. Schematics of stacking sequence of SiC polytypes.

Simulation Procedure. We performed *ab initio* DFT calculations based on the projector augmented wave (PAW) method within the framework of generalized gradient approximation (GGA) using the Vienna Ab Initio Simulation Package VASP [9, 10]. The plane-wave cutoff energy was set to 500 eV and the PW91-GGA functional [11] was adopted.

In the setup the x, y, and z axes are in $[01\bar{1}0]([\bar{1}2\bar{1}])$, $[\bar{2}110](\bar{1}01)$, and $[0001]([111])$, respectively. Shear deformation under zero and nonzero hydrostatic stress is simulated as follows: After finding equilibrium lattice parameters of undeformed crystals by energy minimization under the hydrostatic stress σ_h, shear deformation γ_{zx} is applied to each simulation cell where atomic configuration are relaxed until all the forces are below 0.005 eV/A and normal strains of the cell are adjusted so that normal stress components are within ± 100 MPa from predetermined σ_h.

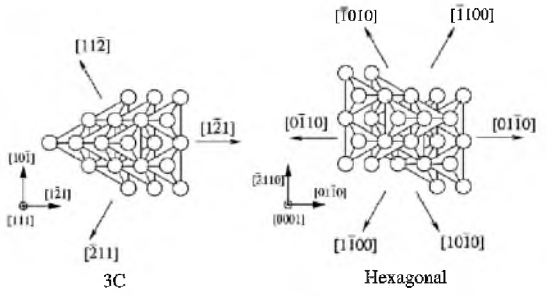

Fig. 2. Schematics of symmetry in shear deformation of 3C and hexagonal SiC crystals.

Results and Discussion. *Stress–Strain Relationship*. Figure 3 shows stress–strain relationships of the cubic and hexagonal polytypes (3C, 2H, 4H, and 6H) obtained by the *ab initio* calculations. The curve of 3C differs from those of the hexagonal polytypes because of the difference in the stacking structure, which is explained in more detail in [8]. Although the stress-strain relations up to $\gamma = 0.2$ are almost identical between the hexagonal polytypes, the polytype structure affects the deformation behavior at higher strains and thus the ideal strength; the maximum stress of 2H is the highest and of 6H the lowest. We find nontrivial effect of the structure of polytypes on the ideal strength τ_{is}; i.e., τ_{is} of 6H (29.83 GPa) is about 10% lower than that of 2H (32.97 GPa). This is obviously due to the stacking pattern (structure) affecting the mechanical properties, which will be discussed later on. The ideal strength of 3C–SiC obtained here, 30.3 GPa, compares well with the value evaluated by the local density approximation (LDA) by Ogata (29.5 GPa [12]).

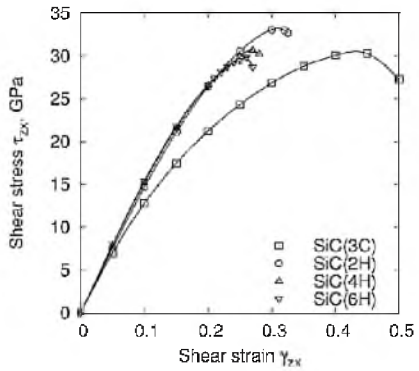

Fig. 3. Stress–strain curves of SiC polytypes.

The ideal (theoretical) shear strength can be correlated with the critical shear strength of dislocation nucleation in a pure crystal. For example, Bahr et al. [13] demonstrated in their study of nanoindentation of tungsten and iron single crystals that the maximum shear stress required for dislocation nucleation shows an excellent agreement with the theoretical shear strength. Ohta et al. [14] devised a sophisticated experimental procedure to evaluate the critical shear stress for dislocation nucleation in silicon, which also compares well with the theoretical strength [15]. To the best or our knowledge, there has been no experimental work extracting the critical shear stress for dislocation nucleation in SiC, but we believe that the value we obtained in this study must be a good prediction. Experimental evaluation of the critical shear stress for dislocation nucleation in SiC is highly desirable although it can be demanding due to the requirement of special techniques such as preparation of specimens with an ideal shape.

Normal Strains and Volume. Changes in normal strains and volume of the SiC polytypes during shear deformation are presented in Fig. 4. The hexagonal polytypes show nearly the same evolution of normal strains with increasing shear strain. In SiC(3C) the evolution of normal strains is different and changes in ε_{xx} and ε_{yy} are more obvious than in the hexagonal polytypes; the former decreases and the latter increases as the shear strain grows. Relative volume, $V/V_0 = (1+\varepsilon_{xx})(1+\varepsilon_{yy})(1+\varepsilon_{zz})$, however, changes similarly both in 3C and the hexagonal polytypes; i.e., the volume decreases with increasing shear strain.

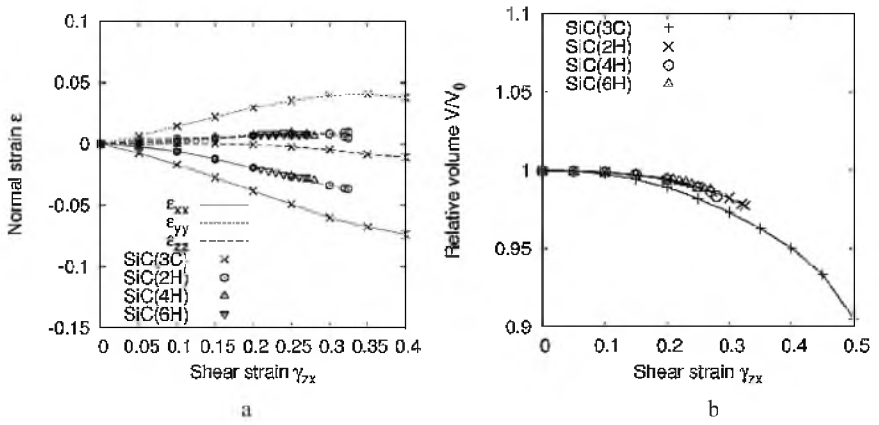

Fig. 4. Changes in normal strains (a) and volume during shear of SiC polytypes (b).

Strain Localization. To investigate the deformation of each Si_4C -tetrahedron lattice, we now show in Fig. 5a the "bond shear strain," γ_b, representing deformation of each atomic bond as in the schematic. In the hexagonal polytypes γ_b differs depending on the layer, signifying that bonds of specific layers deform more than the others. This is analogous to non-uniform deformation or strain localization in inhomogeneous materials (structure). Unlike 3C, inhomogeneous stacking structure intrinsically existing in the hexagonal polytypes causes the strain localization, which affects the ideal strength.

The strain localization shows deviation from the intuitive picture of the deformation that lattices A, B, and C are 'softer' and A', B', and C' are 'stiffer'. In 6H–SiC, while lattices A and B accommodate large and almost identical bond shear strain, lattice C shows a small deformation and its bond shear strain is even smaller than that of C'. This implies that the deformability of the bond is affected by the stacking discontinuity between lattices C and B' (C' and A); i.e., lattice C is stiffened by the overlaying lattice B' (and similarly, C' is softened by A). This effect is seen in the other hexagonal polytypes as well.

The difference in deformation among the layers can be explained by the generalized stacking fault (GSF) energy of the shuffle-set layers shown in Fig. 5b. Here, the lattice over a shuffle-set plane is rigidly shifted along the x direction without atomic relaxation while the lattice below is fixed, and the energy increase as a function of the rigid shift is evaluated (see the schematic in the figure).

The profile of GSF energy depends on the layer, meaning that the bond in each layer has different "deformability." The layer showing lower peak in $0 < x_s < 1$ has a higher deformability, which corresponds to strain localization found in Fig. 5a. The GSF energy profile supports the above-mentioned hypothesis of the mechanism that the deformability of the bond in question is affected by the stacking discontinuity. The GSF energy landscape can be a profile representing the deformability of each bond subject to shear although it does not incorporate the effect of atomistic relaxation.

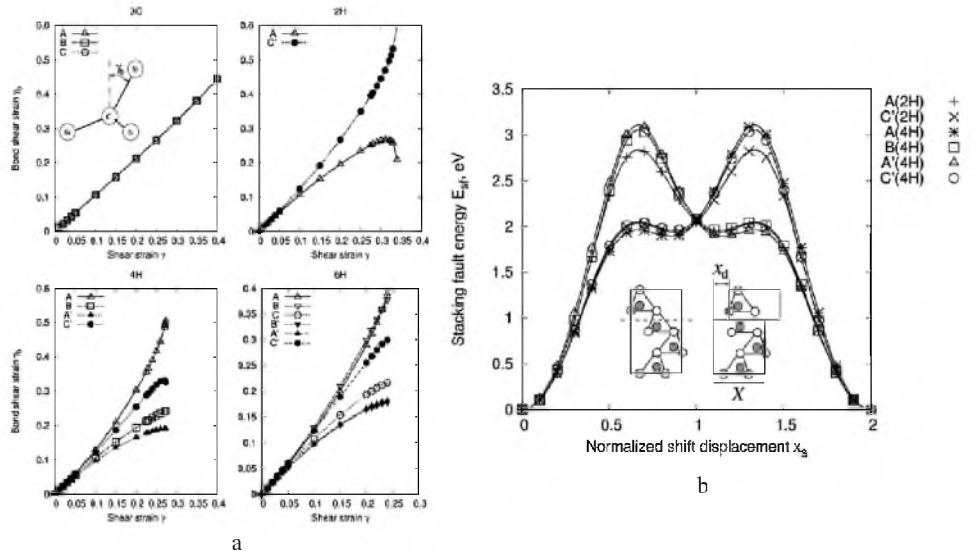

Fig. 5. (a) Evolution of bond shear strain, γ_b. A, B, C and those with a prime denote the tetrahedrons as depicted in Fig. 1. (b) GSF energy landscape of 2H and 4H with a shuffle set being rigidly shifted along the x direction. The abscissa is the shift displacement normalized with respect to the lattice width, $x_s = x_d / X$.

Effect of Pressure. Figure 6 compares the ideal shear strengths of the polytypes under zero and nonzero hydrostatic compression. In the figure, both the abscissa and the ordinate are normalized by τ_{is}^0, the ideal shear strength under no compression. Hydrostatic compression significantly decreases the ideal strength in all the hexagonal polytypes studied here. The response of the ideal shear strength to compression can be explained by the volume change during shear; i.e., the systems contract as the shear strain grows and the compressive normal stress helps the shear deformation. This phenomenon is in contrast with the properties of metals, where, in general, the ideal shear strength increases under compressive pressure [16, 17].

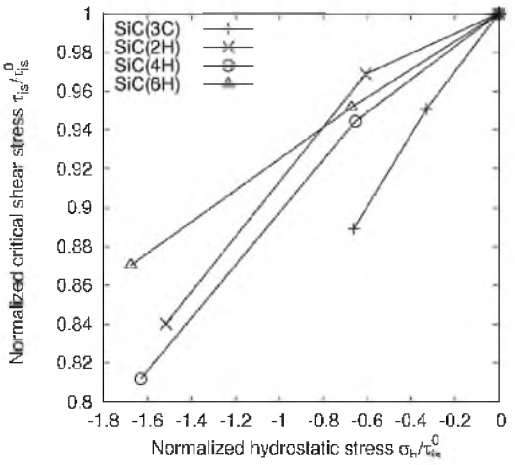

Fig. 6. Ideal shear strength as a function hydrostatic stress. Both abscissa and ordinate are normalized by τ_{is}^0 (the ideal shear strength at $\sigma_h = 0$).

It was demonstrated by Krenn et al. [18] that the effect of compressive stress to the shear strength is important in the interpretation of the critical stress for plastic deformation found in nanoindentation experiments, because the contribution of normal stress components can change the ideal strength in shear. Therefore, our finding here is crucial as it shows that the effect of compressive stress to the shear strength of covalent system can be different even qualitatively from that of metals. As it has been pointed out, the relation between shear and normal stresses exhibits a strong anisotropic character [16] and dependence on atom species [17]. Further extensive studies for various crystals and stress conditions will be necessary to elucidate its mechanism.

Conclusions. We have investigated the ideal shear deformation of SiC polytypes (3C, 2H, 4H and 6H) by means of *ab initio* DFT calculations based on the generalized gradient approximation. The variety of the stacking pattern in the polytypes causes strain localization, which is correlated with the GSF energy profile of each shuffle-set plane, and difference in the ideal shear strength. We also examined the effect of hydrostatic compression to the shear deformation to reveal that the compressive stress decreases the ideal shear strength in all the polytypes studied here, which is in contrast to metals, where in general the ideal shear strength is increased by compression. More extensive studies will be required to elucidate the mechanism of the effect of the normal stress because it can be highly anisotropic and susceptible to the interatomic bonds of the atom species

Acknowledgments. One of the authors (Y.U.) acknowledges financial support from the Grant-in-Aid for Scientific Research of Japan Society of the Promotion of Science (JSPS, No. 1876008).

1. P. T. B. Shaffer, *Acta Cryst. B*, **25**, 477 (1969).
2. W. J. Choyke, H. Matsunami, and G. Pensl, *Silicon Carbide*, Akademie Verlag, Berlin (1997).
3. W. R. L. Lambrecht, B. Segall, M. Methfessel, and M. van Schilfgaarde, *Phys. Rev. B*, **44**, 3685 (1991).
4. P. Kackell, B. Wenzien, and F. Bechstedt, *Phys. Rev. B*, **50**, 17037 (1994).
5. C. H. Park, B. H. Cheong, K. H. Lee, and K. J. Chang, *Phys. Rev. B*, **49**, 4485 (1994).
6. W. Li and T. Wang, *Phys. Rev. B*, **59**, 3993 (1999).
7. S. Ogata, J. Li, N. Hirosaki, et al., *Phys. Rev. B*, **70**, 104104 (2004).
8. Y. Umeno, Y. Kinoshita, and T. Kitamura, *Model. Simul. Mater. Sci. Eng.*, **15**, 27 (2007).
9. G. Kresse and J. Hafner, *Phys. Rev. B*, **47**, 558 (1993).
10. G. Kresse and J. Furthmuller, *Phys. Rev. B*, **54**, 11169 (1996).
11. J. P. Perdew and Y. Wang, *Phys. Rev. B*, **45**, 13244 (1992).
12. S. Ogata, Private Communication (2004).
13. D. F. Bahr, D. E. Kramer, and W. W. Germerich, *Acta Mater.*, **46**, 3605 (1998).
14. H. Ohta, H. Mura, and M. Kitano, *J. Soc. Mater. Sci. Japan*, **45**, 1322 (1996).
15. D. Roundy and M. L. Cohen, *Phys. Rev. B*, **64**, 212103 (2001).
16. S. Ogata, J. Li, and S. Yip, *Science*, **298**, 807 (2002).
17. M. Cerny and J. Pokluda, *Mater. Sci. Eng. A* (in press).
18. C. R. Krenn, D. Roundy, M. L. Cohen, et al., *Phys. Rev. B*, **65**, 134111 (2002).

Received 28. 06. 2007